An Experimental Investigation into the Effect of Bilge Keel Position on Landing Craft Utility Vessels

Eksperimentalno istraživanje o učinku položaja ljuljne kobilice na desantnim pomoćnim brodovima

Sumarsono*
a) Institut Teknologi Sepuluh Nopember, Department of Marine Engineering
b) National Research and Innovation Agency - BRIN
E-mail: sumarsonobpph@gmail.com

Beny Cahyono
Institut Teknologi Sepuluh Nopember, Department of Marine Engineering
E-mail: cak_beny@yahoo.com

Erwandi
National Research and Innovation Agency - BRIN
E-mail: erwandi@brin.go.id

Achmad Baidowi
Institut Teknologi Sepuluh Nopember, Department of Marine Engineering
E-mail: ahmadbai@gmail.com

Baharuddin Ali
National Research and Innovation Agency - BRIN
E-mail: baha002@brin.go.id

DOI 10.17818/NM/2023/4.1
UDK 629.56
629.5.023.21
Original scientific paper / *Izvorni znanstveni rad*
Paper received / *Rukopis primljen:* 13. 1. 2023.
Paper accepted / *Rukopis prihvaćen:* 9. 5. 2023.

Abstract

The issue of energy efficiency in using fossil fuels and reducing the effects of greenhouse gas emissions is an urgent problem. So fuel-saving measures, including in the marine transportation sector, are needed, even if only by a small percentage. Landing Craft Utility (LCU) is a type of sea transport for defense matters that requires the addition of a rolling motion stabilizer for the safety and comfort of the ship, cargo, and passengers. The use of roll-damping devices can affect the increase in the resistance value of the ship and cause an increase in fuel consumption. The bilge keel is a roll-damping device that is suitable for LCU vessels. The experimental study roll decay tests and resistance tests were carried out to determine the effect of the bilge keel placement on roll damping and additional ship resistance. The flow around the vessel's surface was observed with a paint smear test to determine the placement position. The bilge keel installed in the transitional position between the bottom and side hull has the highest total roll damping coefficient, up to 28.57%, compared to the bare hull condition. However, this placement has increased the average resistance up to 8.84%. Alternately, placement close to the draft line has a fairly good roll-damping coefficient of up to 21.27%, increasing the resistance to only 3.66%.

KEY WORDS
bilge keel
experiment model test
paint smear test
resistance test
roll decay test

Sažetak

Pitanje energetske učinkovitosti pri korištenju fosilnim gorivima i smanjivanju djelovanja stakleničkih plinova neodgodiv je problem. Tako su mjere štednje goriva, uključujući i pomorski transportni sector, potrebne, iako u malom postotku. LCU desantno plovilo tip je pomorskoga obrambenog transporta koji zahtijeva dodavanje stabilizatora valjanja zbog sigurnosti i udobnosti broda, tereta i putnika. Korištenje napravama za ublažavanje valjanja u moru može utjecati na povećanje vrijednosti otpornosti broda i potrošnju goriva. Ljuljna kobilica naprava je za ublažavanje valjanja koja je prikladna za LCU brodove. Eksperimentalna studija testova ublažavanja valjanja i testova otpornosti izvršena je kako bi se odredio učinak mjesta ublažavanja valjanja pri ljuljnoj kobilici i dodatna otpornost broda. Promatra se stanje oko površine broda s testom razmaza boje, kako bi se odredio položaj smještaja. Ljuljna kobilica, instalirana na tranzicijskoj položaju između dna i bočnoga trupa, ima najveći ukupan ublažavajući koeficijent, do 28,57%, u usporedbi sa stanjem gologa trupa. Međutim, ova pozicija povećala je prosječnu otpornost do 8,84. Nasuprot tome, smještaj u blizini linije gaza ima prilično dobar koeficijent ublažavanja valjanja do 21,27%, povećavajući otpornost na samo 3,66%.

KLJUČNE RIJEČI
ljuljna kobilica
eksperimentalni pokusni test
test razmaza boje
test otpornosti
test ublažavanja valjanja

1. INTRODUCTION / *Uvod*

The ship will undergo the six degrees of freedom of ship motion in the sea. The rolling motion is the one that affects the comfort of the passengers. The roll motion damper system is part of the ship's free movement damper system. Fin stabilizers, interceptor trim tabs, gyroscopic, and bilge keels are some of the ship's roll-damping systems. External factors, such as the condition of the sea, and internal factors, such as the ship's ability to respond to the movements of the ship itself, influent the ship's stability. Thus, the effectiveness of the roll motion devices is critical for the comfort of the crew and passengers, as well as the ship's safety. Roll motion is an important mode of motion related to vessel stability in which the ship can roll over if a few other coefficients are added [1]. The freedom of movement must be restricted for reasons of safety and comfort. As a result, it requires a component of the roll movement damper system. The Bilge keel is one component that helps

* Corresponding author

dampen roll motion. Due to the simple structure, low production cost, and significant roll-damping effect, this component is widely used in ships and ship-shaped floating bodies.

Bilge keels are recommended as roll dampers because these devices can dampen roll resonance by up to 40% [2], can function effectively in overcoming roll motion over a wide range of sea conditions [3] and are optimal on stationary vessels or at low speeds [4]. Bilge keel is simple to install and completely passive. When a ship encounters high waves, it positively affects anti-rolling performance, especially on ships with a shallow draft [5]. The rotational distance between the tip of the bilge keel and the hull's center is important for its roll damping. The installation on the hull can increase total roll damping because it causes a lot of flow separation and dissipates the ship's kinetic energy. As a result, the popular placement of a 45-degree bilge keel on the hull or at the bottom and side hull transitions may not be the best configuration [6].

Due to the bilge keel installation, the roll damping increases, causing the Response Amplitude Operator (RAO) value to decrease, and, as a result, the ship's motion decreases. When the width of the bilge keel is increased compared to the length, the damping coefficient increases. The wider the bilge keel, rather than the additional length, is more effective at reducing roll motion [7]. Large damping is a vortex-induced phenomenon on ships with flat hull surfaces [8]. The large amplitude response area on flat-hull ships results in greater damping, possibly because the large hull eddies are drawn down the flat hull. Meanwhile, in the low-amplitude response region, the vortices are not pulled down but move 45° to the side [9]. LCU is one type of ship with a dominant flat hull shape, especially in the middle of the Parallel body.

The LCU Vessel serves nearly the same function as the Landing Craft Tank [10] and the Landing Ship Tank. The LCU is a ship designed to transport large-weight units such as tanks or armored vehicles, heavy vehicles and equipment. As a result, the ship will experience static and dynamic loads, which may affect the ship's dynamics. The LCU Vessel research objects have B/T > 3.5 by International Maritime Organization (IMO) provisions for stability. Ships with B/T are classified as special ships for which very few studies are available. Installing of bilge keels on the ship's side affects the increase in the root mean square (RMS) value of rolling at low speeds and the decrease at high speeds. Bilge keels perform effectively at high speeds [11]. The effect of hull shape on a planning hull type ship illustrates the difference in the total coefficient of resistance in various types of planning hulls [12]. Maimun et al. [13] conducted experiments to evaluate the application of the bilge keel on the side of the hull based on variations in dimensions and positions, where the installation affects increasing the security and safety of the ship, despite providing an increase in resistance that is quite large on high-speed ships.

The installation of a bilge keel as a component of the damping system will inevitably increase total resistance. According to Molland et al. [14], the additional resistance caused by the installation typically ranges from 2% to 3% of the total resistance in the bare hull condition. Meanwhile, according to Liu et al. [15], installing a bilge keel reduces roll motion and can increase total resistance by 1.17%. Moreover, according to Maimun et al. [13], the installation resulted in a 14% increase in resistance at high speeds. A high resistance value will require a large ship thrust, which also requires much fuel and produces many carbon emissions. Lowering the resistance can reduce the Energy Efficiency Design Index (EEDI), thus showing clear benefits for a lower EEDI [16]. So, this is an interesting subject, and additional research studies are required to ensure that installing the bilge keel as a damper system does not significantly increase resistance. Previous researchers conducted numerous studies on the bilge keel, but most were done numerically or with Computational Fluid Dynamics (CFD) software to solve the problem. Because of the high cost and completeness of the facilities available, there has been very limited use of experimental methods to determine the bilge keel effect. Generally, the analysis of the resistance test results is consistent with the numerical results [17]. Ship model test experiments provide the most comprehensive data for predicting ship performance. This method still provides more accurate predictions of ship performance than existing to other methods can deliver [18].

A bilge keel is a passive object considered a resistance appendage [19]. This study is an optimization effort to reduce roll motion by increasing the effectiveness of roll damping and searching for bilge keel positions with the least resistance by analyzing four placement variations and trying to increase roll damping while minimizing resistance. The recommended option is the criteria for the placement position with the greatest roll-damping effect and the effect of adding the smallest resistance value.

In this study, bilge keels were placed in several transverse positions with fixed length and width dimensions to investigate the hydrodynamic effect on the resistance value and the hydrodynamic effect on the roll-damping capability of each bilge keel position. The effects were analyzed using the LCU ship model testing method at the Hydrodynamics Laboratory of The National Research and Innovation Agency, Indonesia. Experiments with ship models were carried out in calm water conditions.

2. Methodology / *Metodologija*

2.1. The Geometry of Ship Model Test / *Test geometrije modela broda*

The study was conducted by testing experiments using a scale model of the LCU ship with variations in the placement position of the bilge keel to investigate the hydrodynamic effects on the ship's resistance and roll damping. A flat plate depicting the bilge keel is installed in the selected position, and testing experiments are carried out alternately with several bilge keel position variations. Table 1 shows the dimensions of the ship model used for testing experiments.

Table 1 Model Dimensions
Tablica 1. Dimenzije modela

Item	Symbol	Dimensions	Units
Length water line	LWL	3.357	M
Length between perpendicular	LPP	3.285	M
Breadth	B	0.491	M
Depth	H	0.329	M
Draught	TF	0.080	M
	TA	0.098	M
Displacement	Δ	121.0	Kg
Wide surface area	S	1.919	M^2
Length Centre Buoyancy (from Ap)	LCB from AP	1.424	M
Block Coefficient	CB	0.834	
Scale	λ	33.43	

2.2. Experiment Procedures / *Procedure eksperimenta*

The experiment was carried out in the test pond of the Hydrodynamics Laboratory - National Research and Innovation Agency Indonesia, which measures 234 meters in length, 11 meters in width, and 5.5 meters in depth. This facility has a carriage with a maximum speed of 9 m/s, a high degree of control and speed accuracy, and a towing force load cell dynamometer to determine the resistance value of ship models. Experiments were carried out based on variations in speed and the position of the bilge keel. The model ship (LCU) is drawn at a certain speed in calm water conditions, and the drag force caused by the model ship moving on the water's surface is measured. The model testing procedure was based on The International Towing Tank Conference (ITTC) guidelines for resistance testing, Recommended Procedures, and Guidelines 7.5-02-02-01 [20]. The results of each resistance test measurement on variations of the bilge keel position were compared to determine the effect of the placement on the resistance value [21].

Similarly, the roll decay test was performed in the same pond, with the model in a transverse position in the middle of the pond to avoid back waves caused by the rolling motion of the ship model. Previously, an inclining test procedure was used to determine the distribution of ballast loading based on the position of the center of gravity. The roll decay test is carried out in calm water by applying a few degrees of pressure to the ship model and then releasing it so the ship can roll freely. The test follows the ITTC procedures, Recommended Procedures, and Guidelines 7.5-02-07-04.5 [22] for estimating roll damping.

2.3. Paint Smear Test / *Test razmaza u boji*

The placement of the bilge keel must follow the current flow pattern around the surface of the ship's hull to achieve good performance and has no significant effect on the additional resistance on the ship caused by angular-induced drag on the speed of the ship's motion [23]. A paint smear test was performed in calm water conditions at service speed to determine the current flow. Because the shape of the current flow changes as the speed increases, the paint smear test is carried out at a single operational speed [15], namely a model scale speed of 1,246 m/s. Figure 1 shows the paint smear test. The paint smear test results in forming lines in the paint that are superimposed on each frame station, as shown in Figure 1b. A consistent and inline flow pattern was selected from the flow lines of water currents around the surface of the ship's hull, which was used as the location for placing the bilge keel, as shown in Figure 2. Four locations were chosen to represent the position of the bilge keel as a research object. Each position is given the identities A, B, C, and D to distinguish it.

(a)

(b)

Figure 1 The process of withdrawing the model to the pain smear test. (a) and (b). Flow pattern around the hull of the pain smear test result.

Slika 1. Proces povlačenja modela prema testu trošenja s pomoću razmaza u boji (a) i (b). Uzorak rezultata testa trošenja trupa s pomoću razmaza u boji

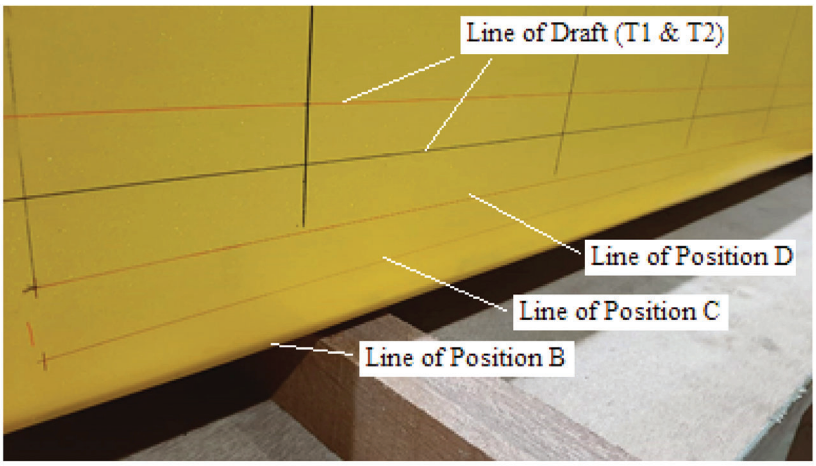

Figure 2 Marking flow pattern lines from the paint smear test as the location for installing the chosen bilge keel.

Slika 2. Markiranje linija uzoraka iz testa razmaza u boji kao lokacija za instaliranje odabrane ljuljne kobilice

Position A represents the bottom surface area at a distance of 0.43B from the centerline. Position B is at the bilge angle. Position C is located on the hull side of the model ship, 0.035 meters from the bottom, and position D is above position C approaching the water draft line. Figures 3 and 4 show the location of the bilge keel, which was chosen based on the pattern of water flow determined by the paint smear test results. In the longitudinal area, the mounting position is parallel to the midship body, around the midship position.

The dimensions of the bilge keel as a research object are based on existing literature, with a length dimension of 0.37L. Meanwhile, the width is 0.03B. Bhattacharyya [23] recommends a bilge keel length of 0.25 to 0.75 of the ship's length. Meanwhile, Sabuncu T. [24], as discussed again by Liu et al. [15], recommends the bilge keel's length of 0.25 to 0.50 of the ship's length and the bilge keel's width of 0.02 to 0.05 of the ship's width. The effect on drag will be minimal if the bilge keel thickness is very thin, such as the sharp tip of a bow ax. Generally, the bilge keel thickness of the ship's hull is very small. With its very thin dimensions, it aims to minimize the effect of adding ship resistance [25].

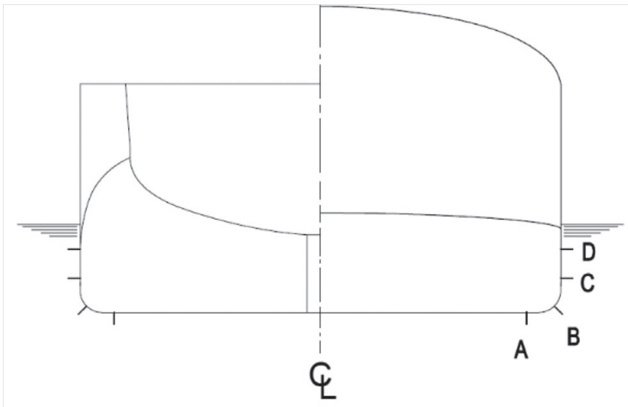

Figure 3a Variations in the placement of the bilge keel based on the results of the paint smear test.
Slika 3a. Varijacije smještaja ljuljne kobilice koje se temelje na rezultatima testa razmaza u boji

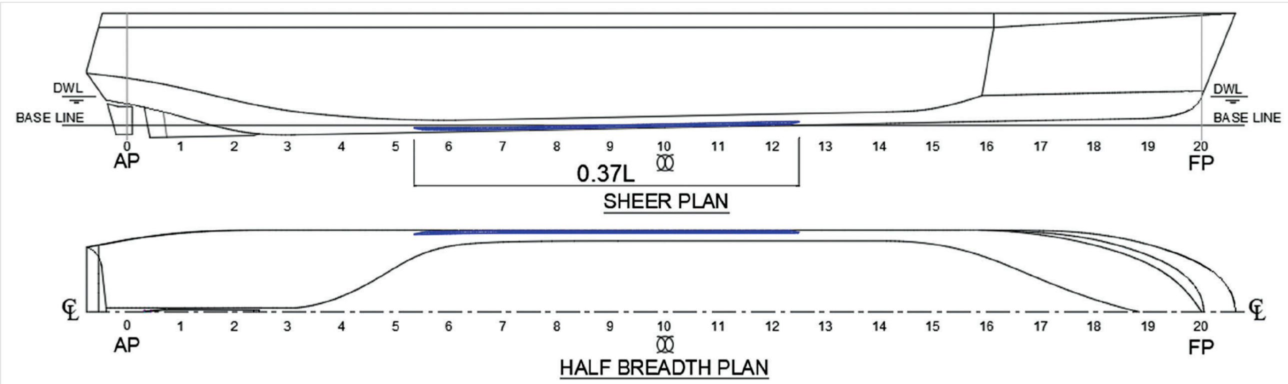

Figure 3b Sheer & halfbreadth plan with dimensions of the bilge keel
Slika 3b Okomiti i polupoprečni presjek s dimenzijama ljuljne kobilice

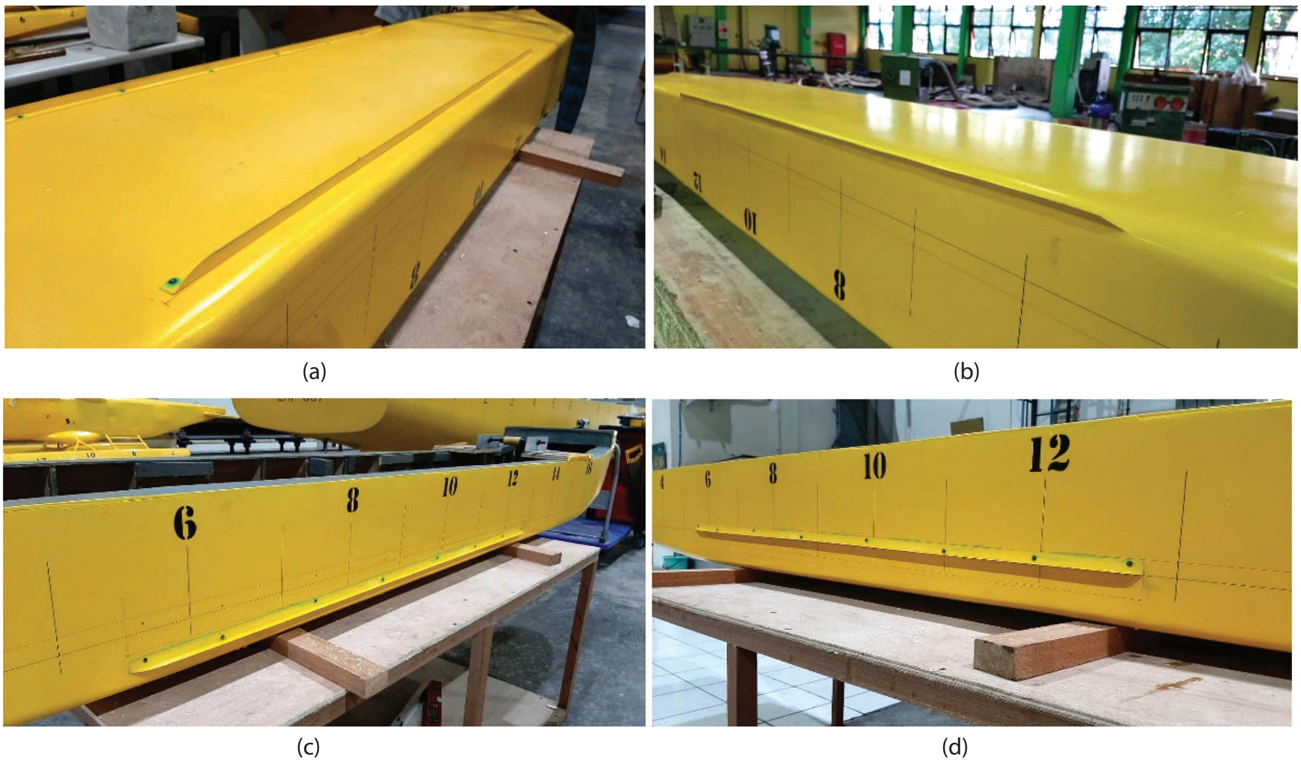

Figure 4 a Position for bilge keel A; b. Position for bilge keel B; c. Position for bilge keel C; d. Position for bilge keel D.
Slika 4 a. Položaj za ljuljnu kobilicu A; Položaj za ljuljnu kobilicu B; c. Položaj za ljuljnu kobilicu C; d. Položaj za ljuljnu kobilicu D

2.4. Roll Decay Test / *Test ublažavanja valjanja*

A series of roll decay tests were performed on a model with a fixed scale at still water conditions to determine the roll damping coefficient [26], [22]. The heel movement is performed by applying pressure to one side of the ship model until it reaches an initial angle (5°, 10°, 15°, 20°, and 25°), then quickly releasing the pressure so that the ship model experiences a roll motion.

Figure 5 shows the process of pressing the initial angle as well as the condition of the free model rolling after the initial corner pressure has been released. Other modes of motion are minimized during the test, and the propagation of the test wave edge causes no back wave disturbance. The experiment was repeated several times at each initial angle. Data recording begins before the model is released to ensure that there is no kick at the time of the release of the initial angle until the roll angle decreases or is less than 0.5. Additional testing was performed to obtain a sufficient number of roll angle peaks.

Data is processed as a roll motion time trace to obtain the roll damping coefficient from the decay test, as shown in Figure 6. This roll decay testing procedure is intended to determine the roll damping coefficient curve and roll period as a function of roll amplitude. According to Lewandowski [27], the decrease in the amplitude of motion in the roll decay test is defined as a polynomial function of the average amplitude as follows:

$$\Delta x = ax + bx_m^2 \quad (1)$$

In Bertin's extinction coefficient N, Δx is defined as a function of the mean squared amplitude x_m^2 as follows:

$$\Delta x = Nx_m^2 \quad (2)$$

So obtained:

$$N = a/x_m + b \quad (3)$$

The least squares method is used to calculate the values of a and b, which are shown in a plot of Bertin's extinction coefficient curve function (x_m, Δx),

Where:

$$\Delta x = |x_{n+1} - x_n| \text{ and } x_m = |(x_{n+1} + x_n)/2| \quad (4)$$

The free decay equation of motion can be written as follows:

$$(M + \Delta M)\frac{d^2x}{dt} + B_1\frac{dx}{dt} + B_2\frac{dx}{dt}\left|\frac{dx}{dt}\right| + kx = 0 \quad (5)$$

Where; $(M + \Delta M)$ is the mass and added mass,
B_1 and B_2 are linear and quadratic motion damping, and
k is a restoring moment.

The integral of equation (5) is the amount of energy lost in motion decay, Froude method, for each half period of the roll. So the equation:

$$B_1\frac{\pi^2}{T}x'^2 + B_2\frac{16}{3T_2}x'^3 - kx'\Delta x = 0 \quad (6)$$

$$\Delta x = \frac{1}{k}\left(B_1\frac{\pi^2}{T}\right)x' + \frac{1}{k}\left(B_2\frac{16\pi^2}{3T_2}\right)x'^2 \quad (7)$$

Equation (7) can be linearized like equation (1). If $x' = x_m$, the coefficients a and b are obtained in the decrement equation of the decay motion in equation (1), respectively:

$$a = \frac{1}{k}\left(B_1\frac{\pi^2}{T}\right) \text{ and } b = \frac{1}{k}\left(B_2\frac{16\pi^2}{3T_2}\right) \quad (8)$$

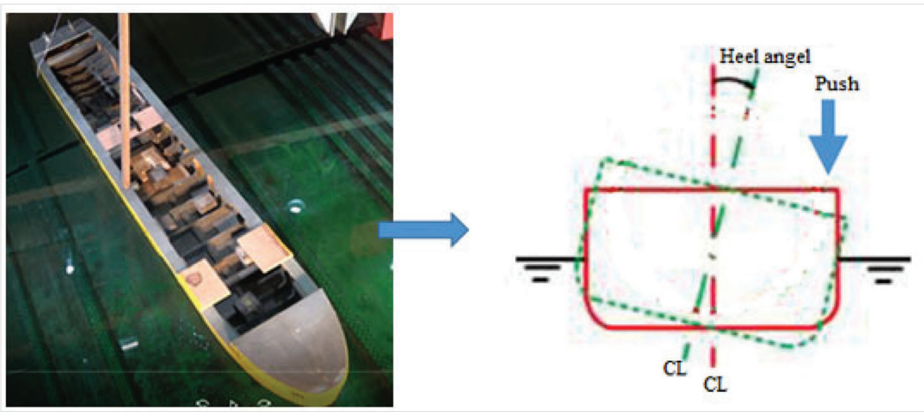

Figure 5 The process of pressing and releasing pressure on the test model.
Slika 5. Proces pritiska i oslobađanja pritiska na testnom modelu

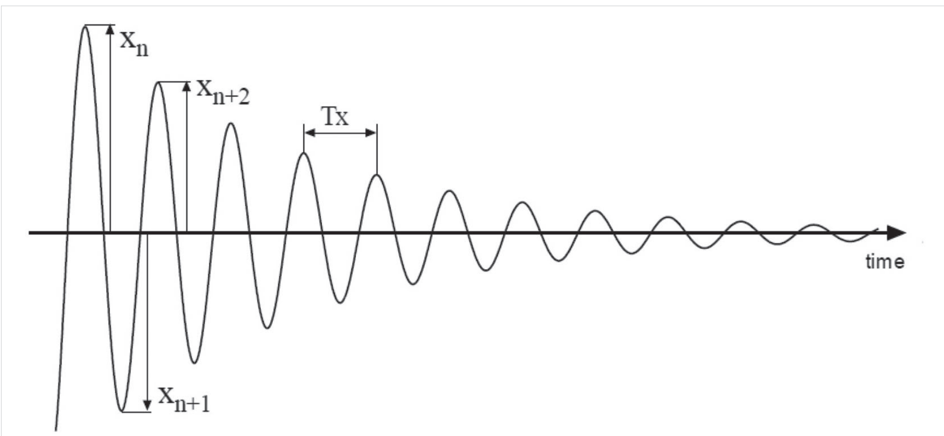

Figure 6 Time trace roll decay test [27].
Slika 6. Test praćenja ublažavanja valjanja

If assumed:

$$x = A\cos\omega t \tag{9}$$

and if $k = \omega^2$, where $m = (M + \Delta M)$ then equation (8) can be written as in equation (10):

$$B_1 = \frac{4}{T}am \text{ and } B_2 = \frac{3}{4}bm \tag{10}$$

A curve of extinction is created from the values of Δx and x_m based on the results of the maxima-minima measurements on the roll decay test. The magnitudes of the linear and quadratic damping coefficients obtained using the least square method are indicated by the values of a and b in equation (1). The linear and quadratic damping values (B_1 and B_2) are obtained from equation (10), which will be used for the numerical prediction of the decay motion as in equation (5).

2.5. Resistance Tests / *Testovi otpornosti*

The resistance test in this experiment aims to determine how much the position of the bilge keel influences the increase in total resistance value. Previously, as described above, a paint smear test was performed to reduce the effect of installing a bilge keel on the total resistance value. As shown in Figure 7, the ship model is mounted on a towing carriage outfitted with a resistance measurement system. The ship model is towed by a Towing Tank carriage, and the force that occurs when the model's speed is stable and the model is only pulled by a resistance dynamometer [28]. The test was repeated several times with the condition of the ship model installed bilge keel according to its respective placement position. The model is towed at a speed close to the operational speed in calm water and full-load draft water conditions according to ITTC procedures. The towing process was carried out alternately for each bilge keel position. Resistance is measured using a Towing Force Dynamometer load cell in conjunction with a data acquisition and analysis recorder system. The testing is carried out by established procedures and is audited regularly by the National Standardization Agency. Moreover, test equipment has been calibrated regularly by both internal and external parties certified and authorized to calibrate equipment. It is done to ensure that the test was performed by the procedure.

Several factors influence resistance value, including hull dimensions, water density, ship speed, water viscosity, gravity, and fluid pressure. The total resistance value is stated in formula (11) with a Froude number to measure the resistance of objects moving in water (12).

$$R_T = \frac{1}{2}\rho . C_T . S . V^2 \tag{11}$$

$$Fn = \frac{V}{\sqrt{gL_{wl}}} \tag{12}$$

Where R_T is the total resistance value, C_T is the total resistance coefficient of water density, S is the wetted surface area, and V is the velocity. The Froude scale distinguishes between full-size and model ships, while the Froude number is in the test.

Total resistance is the sum of several resistance components, namely viscous resistance (R_V), of which friction resistance (R_F) and pressure resistance, wave resistance (R_W), and air resistance are all components [29]. Air resistance is frequently overlooked because its value is insignificant. Total resistance is a function of the Reynolds number and the Froude number [30], which is expressed as a formula:

$$R_{T(R_nF_n)} = R_{V(R_n)} + R_{W(F_n)} = (1+k)_{(F_n)} . R_{F(R_e)} + R_{W(F_n)} \tag{13}$$

The total resistance measured in the resistance test is expressed in the non-dimensional form:

$$C_T = R_T / \left(\frac{1}{2}\rho . S . V^2\right) \tag{14}$$

The extrapolation procedure for the test results data is carried out by following the Froude hypothesis and the law of similarity to convert the data from the model test results into full scale:

$$R_{W_s} = R_{W_m} . \lambda^3 . \frac{\rho_s}{\rho_m} \tag{15}$$

With the provision of:

$$V_s = V_m\sqrt{\lambda}$$

The proportionality factor, also known as the form factor (1+k), is used to account for the effect of the three-dimensional hull shape. The extrapolation method raises the scale of the resistance results:

$$R_s = \left(R_m - R_{F_m}(1+k)\right)\lambda^3\frac{\rho_s}{\rho_m} + R_{F_s}(1+k) + R_{allowance}$$

$$R_s = (R_m - F_D)\lambda^3\frac{\rho_s}{\rho_m} \tag{16}$$

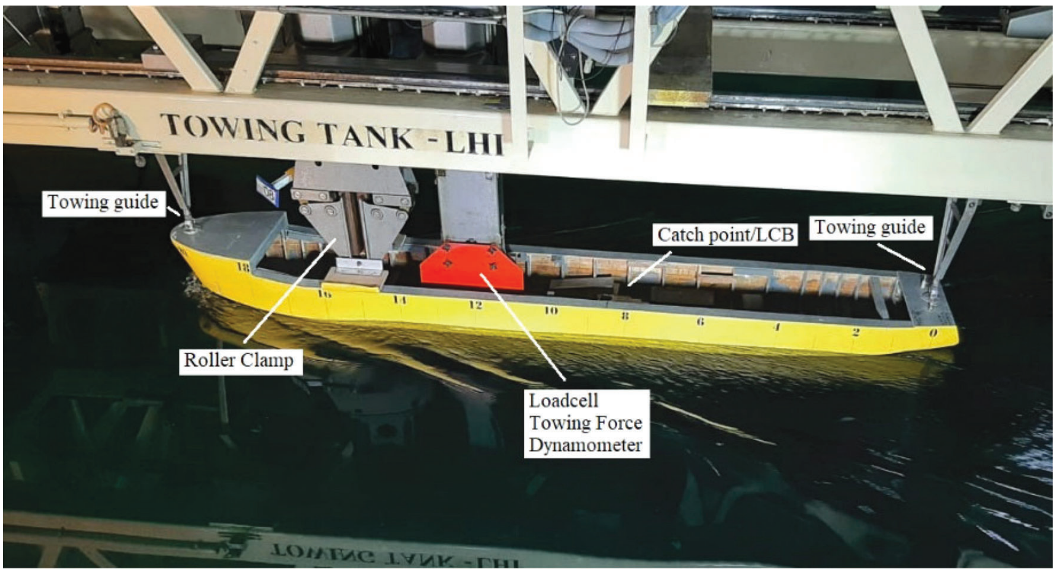

Figure 7 Resistance testing installation scheme.
Slika 7. Shema instalacije testa otpornosti

Where

$$F_D = 0.5\rho_m V_m^2 S_m (1+k)\left(C_{F_m} - C_{F_s}\right) - \frac{\rho_m}{\rho_s} R_{allowance}/\lambda^3$$

$$F_D = 0.5\, \rho_m\, V_m^2\, S_m \left\{(1+k)\left(C_{F_m} - C_{F_s}\right) - \frac{\rho_m}{\rho_s} C_A\right\} \qquad (17)$$

From the above equation, the resistance coefficient value is then sought with the following equation:

$$C_T = C_{Tm} - (1+k)\,.\,(C_{Fs} - C_{Fm})\,.\,C_A \qquad (18)$$

$$C_{Fs} = \frac{0.075}{(log10\; R_n - 2)^2} \qquad (19)$$

$$C_A = 0.006(Lwl + 100)^{-0.16} - 0.00205 \qquad (20)$$

$$C_{Tm} = \frac{R_{Tm}\,.\;9.81}{0.5\rho S V^2} \qquad (21)$$

Where

C_T = Coefficient of ship resistance, C_{Tm} = Coefficient of model resistance,

(*1+k*) = Form factor, C_{Fs} = Coefficient of ship friction,

C_{F_m} = Coefficient of model friction, and

C_A = The additional resistance coefficient for ship model correlation.

Furthermore, the Prohaska method can be used to find out the value of the hull form factor [31]. This method is based on ship model testing, where a ship model is towed in a towing tank by the value of Froude Number (*Fn*) in the range 0.1 to 0.2 to obtain the resistance coefficient of the C_{Tm} model and the friction coefficient of the C_{F_m} model. So that a plot can be made, as shown in Figure 8. The form factor value obtained is at the intersection of the C_T/ C_F and $F_n^{\,4}/ C_F$ axes.

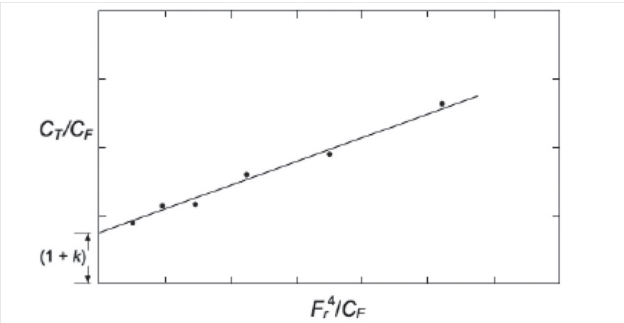

Figure 8 The plot of Form factor (1 + k) using the Prohaska method.
Slika 8. Prikaz čimbenika Form (1+k) koristeći se Prohaska metodom

In full-scale resistance, the effective power is defined as follows:

$$P_E = R_s\,.\,V_s \qquad (22)$$

Where P_E = Efectif Power, R_s = Ship Resistance, and V_s = Speed.

3. RESULTS & DISCUSSION / *Rezultati i rasprava*

3.1. Coefficient of Roll Damping / *Koeficijent ublažavanja valjanja*

Figure 9 represents the roll decay test results' roll period for ship models with and without bilge keels with different placement positions. The figure shows that the roll period has no significant difference in all bilge keel position variations. Whereas the period for the bare hull roll condition is 0.90102 seconds, the period at full scale is 5.2096 seconds, the shortest roll period of all variations. The test results show that almost the same roll period is possible because the center of gravity of the VCG (Vertical Centre of Gravity) and the radius of the gyration of the roll is the same. Differences can occur due to the length of the radius or distance of the bilge keel position from the center of gravity, both of which can affect the damping moment induced by the bilge keel [32].

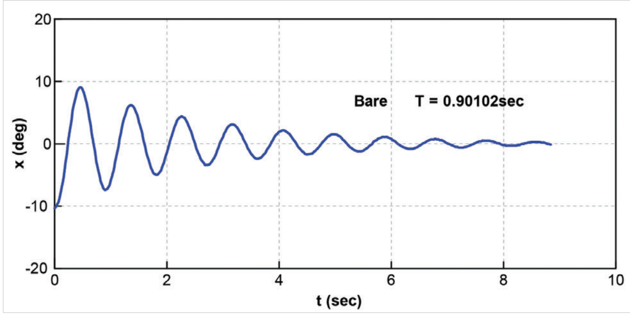

(a)

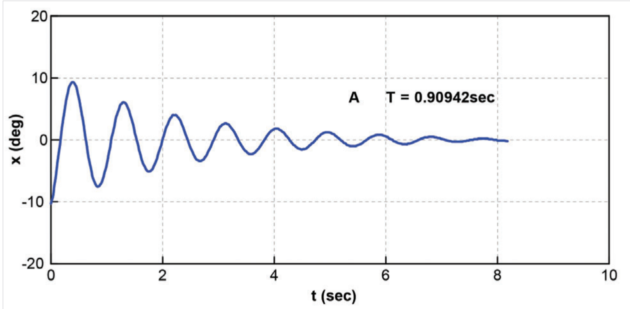

(b)

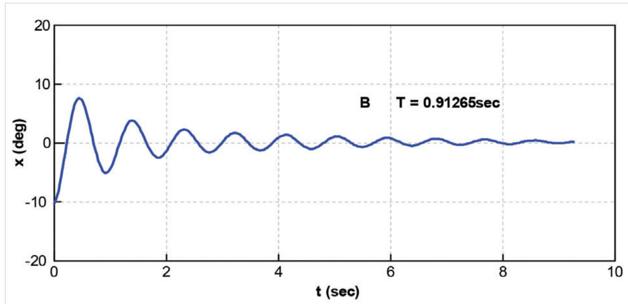

(c)

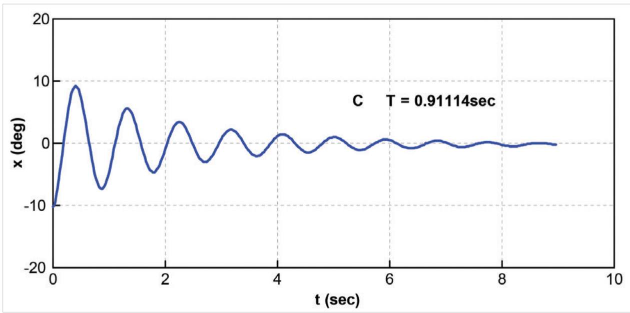

(d)

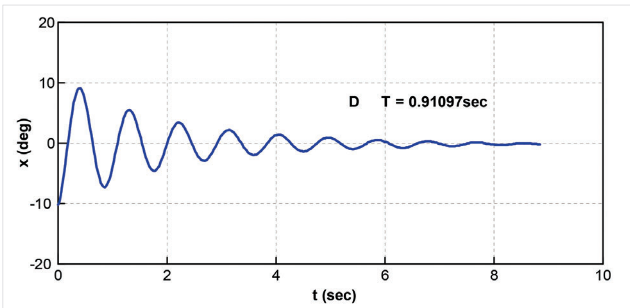

(e)

Figure 9 Time trace roll decay test at each position of bilge keel placement (a). Condition of the bare hull, (b). Position A, (c). Position B, (d). Position C, and (e). Position D.

Slika 9. Test praćenja ublažavanja valjanja na svakom položaju smještaja ljuljne kobilice (a). Uvjeti gologa trupa, (b). Položaj A, (c). Položaj B, (d) Položaj C i (e). Položaj D

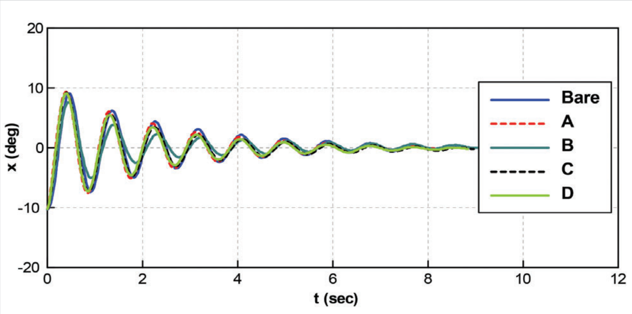

Figure 10 Time history of decay tests for bare hull models and models with bilge keels in positions A, B, C, and D.
Slika 10. Vremenski pregled testa ublažavanja pri golom trupu i modela s ljuljnim kobilicama na položajima A, B, C i D

The bilge keel also affects friction and lift forces, decreasing rolling angular velocity [33]. Figure 10 shows the roll decay test's time history for the bare hull model condition and the variations in the different bilge keel positions. The roll period of variation B is greater than that of the other variations, as shown in the figure.

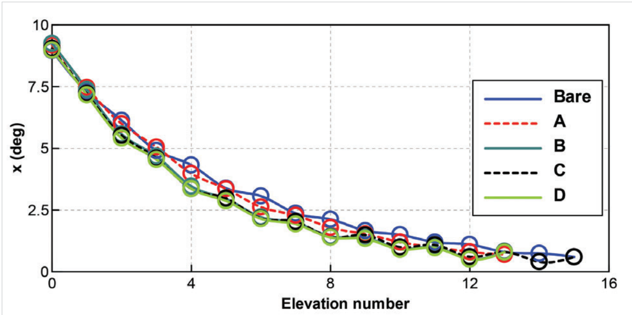

Figure 11 Elevation-damping trend.
Slika 11. Trend povećavanja ublažavanja

Figure 11 shows the elevation-damping trend. It demonstrates that the damping time trend for ship models with bilge keels reduces rolling faster than ship models without them. Variations in the placement position of the bilge keel B show that the ship model returns to its original state (equilibrium) fastest of all variations.

Figures 12 and 13 show the extinction curve derived from the roll decay test results. Figure 12 is the result of using the Froude method to fit the data obtained from the roll decay test results. The values of and in the curve of extinction figure are the coefficients of the linear and quadratic roll damping components, respectively. Figure 13 shows the value of Bertin's coefficient or the *N* coefficient obtained by solving Equation (3).

Figure 12 represents a graph of the curve of the maxima and minima values from the roll decay test results at each variation in the position of the bilge keel placement as in equation (1). The curve line on the bare hull condition ship model is at the bottom and shows a decrease in motion amplitude on a small roll decay test. In variation B, however, the roll decay amplitude reduction curve is very dominant. It shows that the placement of the bilge keel has the highest damping coefficient in the variation of position B. Variation D can be the alternative option for the placement position because it has a lower extinction curve than variation B but higher than the other variations.

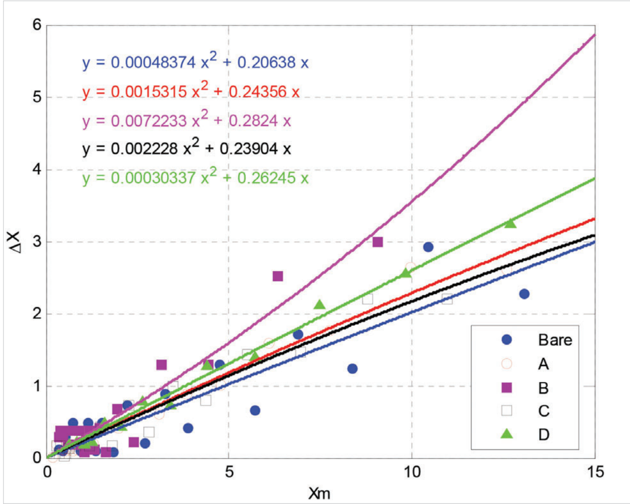

Figure 12 Fitting the roll damping coefficient for each bilge keel position variation.
Slika 12. Uređivanje koeficijenta ublažavanja valjanja za svaku varijaciju ljuljne kobilice

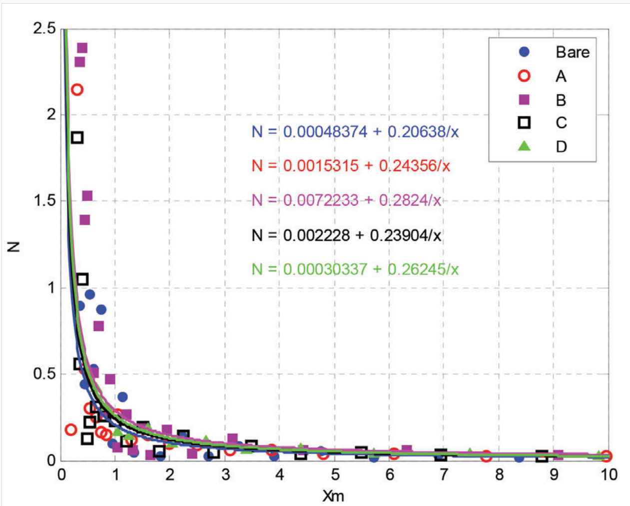

Figure 13 N coefficients of roll damping for each variation in bilge keel position.
Slika 13 N koeficijent ublažavanja valjanja za svaku varijaciju položaja ljuljne kobilice

Table 2 The decay damping coefficient of Froude method.
Tablica 2. Koeficijent ublažavanja valjanja s pomoću metode Froude

Bilge Position	*Tn* (sec)	a	b
Bare hull	0.90102	0.20638	0.000484
Position A	0.90942	0.24356	0.001532
Position B	0.91265	0.28240	0.007223
Position C	0.91114	0.23904	0.002228
Position D	0.91097	0.26245	0.000303

Table 2 shows the results of the roll decay test for each roll damping component. The table shows that variations in the position of different bilge keel placements indicate different roll-damping coefficient values for the linear and quadratic components. Position B variation has linear and quadratic component values that are very dominant compared to other variations. While the D variation has a fairly large linear component value, it has a low quadratic component value. The difference in total coefficient value between the bare hull condition and the placement in position B is estimated at 28.57%. Moreover, the difference in the total value of the coefficient with variations in the placement of the bilge keel in position D is estimated at 21.27%.

Table 3 The decay damping coefficient of relative decrement method.
Tablica 3. Koeficijent ublažavanja valjanja metodom relativnoga smanjenja

Bilge Position	p	q
Bare hull	0.30018	0.014691
Position A	0.37992	0.010432
Position B	0.28504	0.058139
Position C	0.32089	0.019093
Position D	0.45822	0.005766

To obtain the damping values B_1 and B_2 from the relative damping method, the following equations can be used:

$$B_1 = 2p\frac{m}{T_d} \quad \text{and} \quad B_2 = \frac{3}{8}\, qm$$

Table 4 Roll damping B_1 and B_2.
Tablica 4. Ublažavanje valjanja B_1 i B_2

	B_1		B_2	
Bilge Position	Froude	Relative	Froude	Relative
Bare hull	$0.9162\,.\,m$	$0.66632\,.\,m$	$0.000363\,.\,m$	$0.005509\,.\,m$
Position A	$1.0713\,.\,m$	$0.83552\,.\,m$	$0.001149\,.\,m$	$0.003912\,.\,m$
Position B	$1.0507\,.\,m$	$0.62522\,.\,m$	$0.009877\,.\,m$	$0.021802\,.\,m$
Position C	$1.0494\,.\,m$	$0.70437\,.\,m$	$0.001671\,.\,m$	$0.007160\,.\,m$
Position D	$1.1524\,.\,m$	$1.00600\,.\,m$	$0.000228\,.\,m$	$0.002162\,.\,m$

where $m = (M + \Delta M)$

In this study, the damping calculations using the Froude energy method is validated by the relative decrement method referring to studies conducted by Kim et al. [34]. As shown in Table 4, the damping value between the Froude energy and relative decrement methods is slightly discrepency.

3.2. Comparison of Resistance Value / *Usporedba vrijednosti otpornosti*

Figure 14 shows the resistance test results in the bare hull and bilge keel installation conditions in each variation of placement position. The resistance was measured at a model test speed of 0.89 - 1.60 m/s, or 10 - 18 knots on the full scale. The resistance test results on bare hull conditions show the lowest graphic trend. This result is understandable, given that the test model lacks the bilge keel appendages. The figure also shows that variations in the placement in position D have the lowest trend of resistance test results in the test conditions with the installation of bilge keel appendages. While in position B shows the greatest trend of the value of the resistance testing results

Table 5 shows the data of each bilge keel placement variation's ship model resistance test results. From the results of the ship model resistance test, the calculation of the ship model resistance coefficient is then used in the extrapolation calculation to obtain ship resistance data.

Table 6 presents the results of full-scale ship resistance data for each bilge keel placement variation obtained by extrapolation calculation method using form factor. The Prohaska method is used to obtain the value of the hull form factor so that a form factor value of 1.372 is obtained. The difference in average resistance values between positions B and D is 4.76%, which can make position D an alternative option for bilge keel placement when the results of the damping roll test are also considered. Compared to bare hull conditions, adding the resistance value due to the placement in position D results in an average difference of 3.66%. While the addition of the resistance value due to the placement of the bilge keel in position B compared to the average bare hull condition is 8.84%.

Table 5 Resistance test results of ship model
Tablica 5. Rezultati testa otpornosti na uzorku broda

Vs	Vm	Fn	Bare hull Condition		Position A		Position B		Position C		Position D	
			Rm	Ctm	Rm	Ctm	Rm	Ctm	Rm	Ctm	Rm	Ctm
knots	m/s		N	$*10^5$	N	$*10^5$	N	$*10^5$	N	$*10^5$	N	$*10^5$
10	0.890	0.155	3.68	485	3.73	491	3.76	493	3.73	492	3.7	487
11	0.979	0.171	4.44	483	4.54	495	4.56	494	4.60	500	4.49	488
12	1.068	0.186	5.32	486	5.51	503	5.50	504	5.60	512	5.42	495
13	1.157	0.202	6.44	502	6.71	522	6.73	523	6.79	529	6.62	515
14	1.246	0.217	7.97	535	8.27	555	8.17	547	8.26	555	8.26	555
15	1.335	0.233	9.84	576	10.15	594	9.92	588	10.01	586	10.24	599
16	1.424	0.248	11.96	615	12.31	633	12.71	646	12.08	621	12.38	637
17	1.513	0.264	14.40	656	14.81	675	15.06	693	14.52	662	14.76	672
18	1.602	0.279	17.18	698	17.66	718	17.77	723	17.39	707	17.34	705

Table 6 Resistance in all variations of the bilge keel position

Tablica 6. Otpor u svim varijacijama položaja ljuljne kobilice

Vs	Rs Barehull	Rs Position A	Rs Position B	Rs Position C	Rs Position D
knots	*kN*	*kN*	*kN*	*kN*	*kN*
10	75	76.8	81.3	77.1	75.6
11	92.4	96.5	101	98.5	94.2
12	114	121	126	124	117
13	143	154	160	157	150
14	188	199	201	199	199
15	245	257	261	252	260
16	311	324	343	315	327
17	388	404	429	393	402
18	478	496	512	486	484

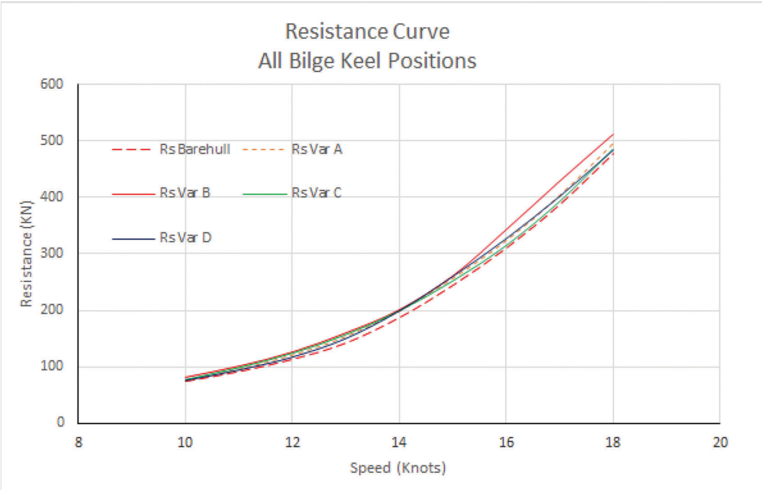

Figure 14 Total resistance graph based on resistance test results at various test speeds and bilge keel position variations.

Slika 14. Grafikon ukupne otpornosti koji se temelji na rezultatima testa otpornosti pri različitim testnim brzinama i varijacijama položaja ljuljne kobilice

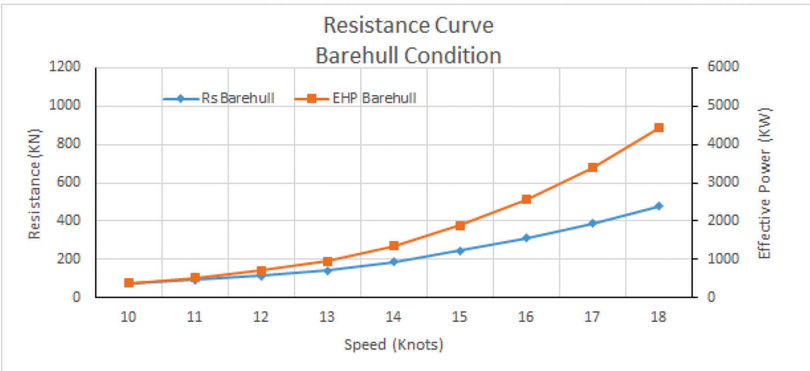

(a)

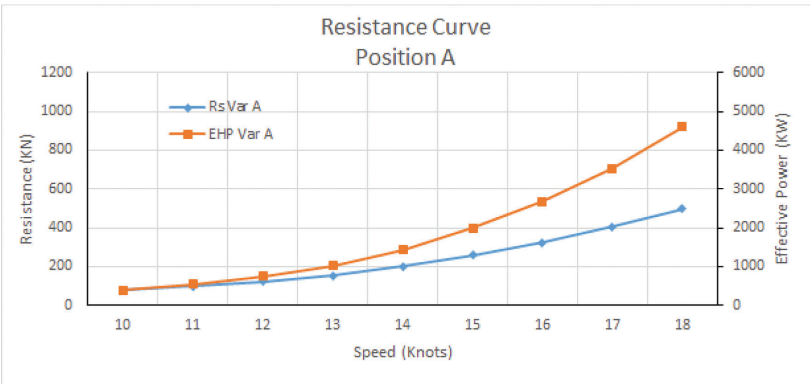

(b)

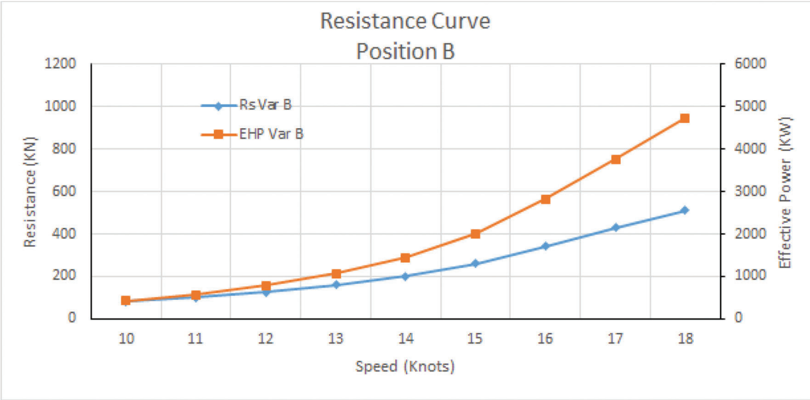

(c)

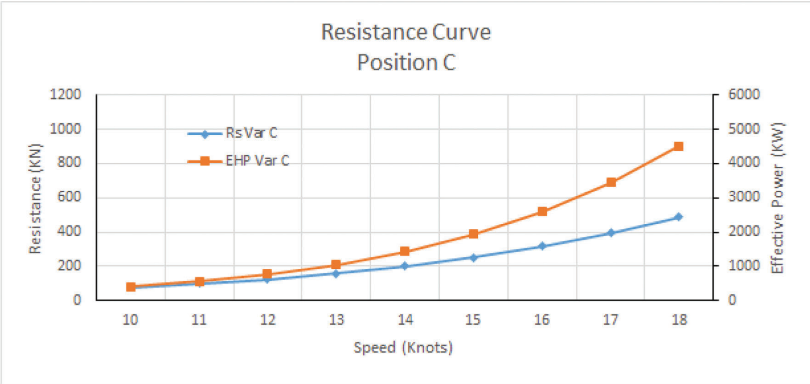

(d)

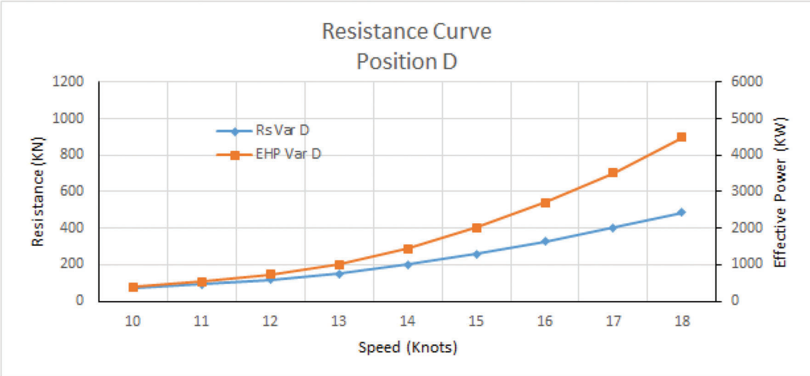

(e)

Figure 15 Resistance and effectiveness at each position of the bilge keel (a). Condition of the bare hull, (b). Position A, (c). Position B, (d). Position C, and (e). Position D.

Slika 15. Otpornost i djelotvornost pri svakom položaju ljuljne kobilice (a). Uvjeti gologa trupa, (b). Pozicija A, (c). Pozicija B, (d). Pozicija C i (e). Pozicija D.

Figure 15 represents the effective power required to move the ship to reach the speed at each resistance result for each bilge keel placement position. At cruising or service speed of 16 knots, the difference in effective power between position B with position D is 4.68%, and the difference with position C which has the smallest resistance value is 8.59% or 223 kW. At a maximum speed of 18 knots, the difference in effective power between variation position B, which has the highest resistance value, and variation D, which has the lowest resistance value, is 5.71% or 256 kW.

Table 7 Effective Horse Power in all variations of the bilge keel position

Tablica 7. Efektivna konjska snaga u svima varijacijama pozicije ljuljne kobilice

Vs	EHP Barehull	EHP Position A	EHP Position B	EHP Position C	EHP Position D
knots	*kW*	*kW*	*kW*	*kW*	*kW*
10	386	395	418	396	389
11	523	546	570	557	533
12	701	746	779	767	725
13	959	1027	1069	1050	1005
14	1354	1437	1451	1434	1435
15	1892	1984	2012	1941	2009
16	2560	2671	2819	2596	2693
17	3397	3532	3755	3437	3515
18	4428	4597	4740	4502	4484

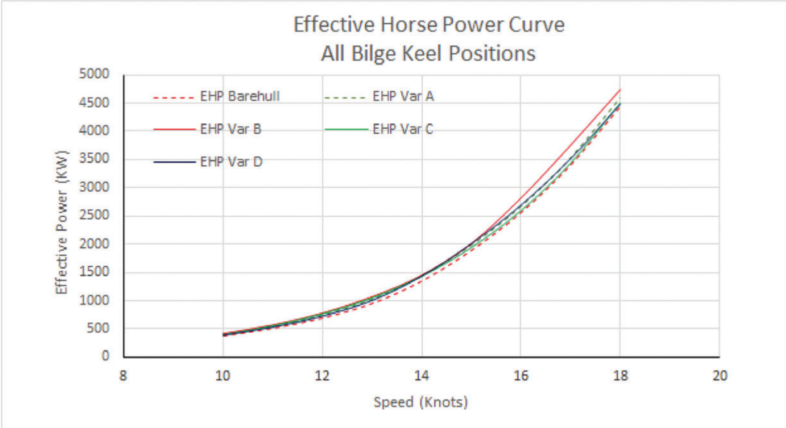

Figure 16 Effective Horse Power.
Slika 16. Efektivna konjska snaga

Table 7 presents the Effective Horse Power data for each bilge keel placement variation. Position B significantly impacts the resistance value at all speeds (10 knots to 18 knots). As a result, the effective power required to move the ship is the greatest on average compared to variations in the position of other placements. While the minimum average effective power is in position C. This bilge keel is placed on the side hull close to the bilge area. At a speed of 16 knots, the effective power requirement in variation B is 2819 kW. At the same time, the effective power requirement without it is 2560 kW. The effective power requirements of position B increase by up to 10.12% compared to conditions without it. When in position C, the effective power requirement at an operational speed of 16 knots, compared to the condition without the bilge keel, increases by 36 kW or 1.41%. The effective power in each variation is shown in Figure 16.

4. CONCLUSIONS / *Zaključci*

1. In the study, the experiment paint smear test is very helpful in the optimization process of selecting the bilge keel placement position. Observing the flow around the hull obtained from the paint smear test aids in minimizing the effect of increasing the resistance value.
2. The roll decay tests produced linear and quadratic roll damping coefficients for each bilge keel placement position variation. The roll damping coefficient is dominated by the variation of position B, which is the placement position at the bilge angle or the bottom and side hull transitions. Position B has a difference in the value of the roll damping coefficient up to 28.57% compared to the condition without the bilge keel. Moreover, position D, where the bilge keel placement is close to the draft line, has a roll-damping coefficient of up to 21.27%.
3. Position B is not only dominant in the roll damping coefficient, but also has the highest resistance results among all bilge keel placement variations. Position B has an increase in average resistance of up to 8.84% when compared to the condition without the bilge keel. Under the ship's operational speed of 16 knots, it requires an effective power of 2819 kW. There is an increase in the effective power requirement of 259 kW or 10.12% compared to the condition without a bilge keel. The lowest increase in average resistance value is position C with an average increase of up to 3.3% and an increase in effective power requirement at an operational speed of 16 knots of 36 kW compared to the condition without bilge keel. There was an increase of only up to 1.41%.
4. Position D can be an alternative because it has a large enough roll damping coefficient of 21.27% but has a fairly small increase in the average resistance value of up to 3.66%, and the effective power requirement at operational speed is 133 kW compared to the condition without bilge keel.

Author Contributions: Sumarsono: conceptualization, methodology, calculations, formal analysis, writing – original draft, writing – review, and editing, visualization; Beny Cahyono: conceptualization, methodology, and review; Erwandi: methodology, formal analysis, and review; A. Baidowi: review and editing; B. Ali: experiments, and numerical data calculation.

Funding: This study was funded under the Degree by Research is under research scheme by the National Research and Innovation Agency, No: SP/141/BPPT/08/2021.

Conflict of interest: The authors state that there is no conflict of interest.

Acknowledgement: The authors acknowledge the facilities, scientific and technical support form Hydrodynamics Laboratory, National Research and Innovation Agency.

REFERENCES / *Literatura*

[1] Kobyliński, L. (2007). System and risk approach to ship safety, with special emphasis of stability. *Archives Of Civil And Mechanical Engineering*, VII (Foundation for Safety of Navigation and Environment Protection). https://doi.org/10.1016/S1644-9665(12)60228-3

[2] Ali, B., Katayama, T. & Ikeda, Y. (2004). Roll damping characteristics of fishing boats with and without drift motion. *International Shipbuilding Progress*, 51(2-3) (The Stability of Ships and Ocean Vehicles), 237-250. https://shipstab.org/files/Proceedings/STAB/STAB2003/Papers/Paper%2051.pdf

[3] Ikeda, Y. (2004). Prediction Methods of Roll Damping of Ships and Their Application to Determine Optimum Stabilization Devices. *Marine Technology*, 41(2), 89-93. https://doi.org/10.5957/mt1.2004.41.2.89

[4] Ferrari Jr., J. A., A. Ferreira, M. D. (2002). Assessment of the Effectiveness of the Bilge Keel as an Anti-Roll Device in VLCC-Sized FPSOs. *Proceedings of the International Society of Offshore and Polar Engineers Conference*, 12, 107-113. https://onepetro.org/ISOPEIOPEC/proceedings-abstract/ISOPE02/All-ISOPE02/ISOPE-I-02-018/8256

[5] Choiriya, L. & Aryawan, W. D. (2013). Desain Bilge Keel pada Shallow Draft Bulk Carrier. *Jurnal Teknik Pomits*, 2(1), 1-5. https://docplayer.info/136826923-Desain-bilge-keel-pada-shallow-draft-bulk-carrier.html

[6] Jiang, Y., Ding, Y., Sun, Y., Shao, Y. & Sun, L. (2020). Influence of bilge-keel configuration on ship roll damping and roll response in waves. *Ocean Engineering*, 216. https://doi.org/10.1016/j.oceaneng.2020.107539

[7] Hendratmoko, H., Hasanudin, Utama, I. K. A. P. (2012). Studi Eksperimen Pengaruh Lunas Bilga Terhadap Gerakan Rolling. *Jurnal Teknik ITS*, 1(1), G94-G97. https://ejurnal.its.ac.id/index.php/teknik/article/view/362%0Ahttps://ejurnal.its.ac.id

[8] Oliveira, A. C. & Fernandes, A. C. (2011). Roll damping of flat-bottom hulls: Critique of the quadratic reason. *Marine Technology and Engineering*, 1 (Marine Environment, Dynamics and Hydrodynamics). https://www.researchgate.net/publication/288050382_Roll_damping_of_flat-bottom_hulls_Critique_of_the_quadratic_reason

[9] Fernandes, A. C. & Oliveira, A. C. (2009). The roll damping assessment via decay model testing (new ideas about an old subject). *Journal of Marine Science and Application*, 8(2), 144-150. https://doi.org/10.1007/s11804-009-8107-z

[10] Yudo, H., Yulianti, S., Pratiwi, O. R. & Tuswan. (2021). The conversion strategy from landing craft tank into livestock carrier: An overview of technical evaluation and economical benefit. *Brodogradnja*, 72(3), 29-44. https://doi.org/10.21278/brod72303

[11] Widyatmoko, A., Samuel, Manik, P. & Trimulyono, A. (2021). Analisis Pengaruh Jumlah Bilge Keel terhadap Gerakan Rolling pada Kapal Patroli 14 m. *Warta Penelitian Perhubungan*, 33(1), 1-10. https://doi.org/10.25104/warlit.v33i1.1667

[12] Utama, I. K. A. P., Sutiyo, Suastika, I. K., Sulisetyono, A., Hasanudin, Hermawan, Y. A. & Aryawan, W. D. (2021). Resistance Analysis of Rescue Boat in Calm Water Condition. *IOP Conference Series: Materials Science and Engineering*, 1052, 012062. https://doi.org/10.1088/1757-899x/1052/1/012062

[13] Maimun, A., Priyanto, A., Wong, K. S., Pauzi, M. & Rafiqul, M. (2009). Effects of side keels on patrol vessel safety in astern waves. *Ocean Engineering*, 36(3-4), 277-284. https://doi.org/10.1016/j.oceaneng.2008.12.003

[14] Molland, A. F., Turnock, S. R. & Hudson, D. A. (2017). *Ship resistance and propulsion*. 2nd ed. Cambridge University Press. https://doi.org/10.1017/9781316494196

[15] Liu, W., Demirel, Y. K., Djatmiko, E. B., Nugroho, S., Tezdogan, T., Kurt, R. E., Supomo, H., Baihaqi, I., Yuan, Z. & Incecik, A. (2018). Bilge keel design for the traditional fishing boats of Indonesia's East Java. *International Journal of Naval Architecture and Ocean Engineering*, 11(1), 380-395. https://doi.org/10.1016/j.ijnaoe.2018.07.004

[16] Luhulima, R. B., Sutiyo, S. & Utama, I. K. A. P. (2022). The Resistance and EEDI Analysis of Trimaran Vessel with and without Axe-bow. *Naše more*, 69(3), 132-142. https://doi.org/10.17818/NM/2022/3.1

[17] Hu, J., Zhang, Y., Wang, P. & Qin, F. (2020). Numerical and experimental study on resistance of asymmetric catamaran with different layouts. *Brodogradnja*, 71(2), 91-110. https://doi.org/10.21278/brod71206

[18] Babicz, J. (2015). *WÄRTSILÄ Encyclopedia of Marine and Energy Technology: Model Tests*. 2nd ed. WÄRTSILÄ CORPORATION. https://www.wartsila.com/encyclopedia/term/model-tests

[19] Mandru, A. & Pacuraru, F. (2021). The effect of appendages on ship resistance. *IOP Publishing*, 1182 (Materials Science and Engineering). https://doi.org/10.1088/1757-899X/1182/1/012041

[20] ITTC. (2011). Recommended Procedures and Guidelines – Resistance Test. *The International Towing Tank Conference*, *7.5-02-02-01*. https://ittc.info/media/1217/75-02-02-01.pdf

[21] Suwarni, E. & Utama, I. K. A. P. (2018). Analisis Komparatif Hambatan Kapal Katamaran Pada Perairan Dangkal, Medium Dan Dalam (Comparative Analysis of Catamaran Resistance in Shallow, Medium and Deep Waters). *Wave: Jurnal Ilmiah Teknologi Maritim*, 7(2), 37-42. https://doi.org/10.29122/jurnalwave.v7i2.3199

[22] ITTC. (2021). Recommended Procedures and Guidelines: Estimate of Rolling Damping Procedure. *International Towing Tank Conference*, *7.5-02-07-04.5*. https://www.ittc.info/media/9759/75-02-07-045.pdf

[23] Bhattacharyya, R. (1978). *Dynamics of marine vehicles*. John Wiley & Sons Incorporated. https://scholar.google.com/scholar?hl=id&as_sdt=0%2C5&q=Dynamics+of+marine+vehicles+Bhattacharyya&btnG=

[24] Sabuncu, T. (1983). *Gemi hareketleri (İTÜ)*. Istanbul Teknik Universitesi. https://scholar.google.com/scholar?hl=id&as_sdt=0%2C5&q=Gemi+hareketleri+%28%C4%B0T%C3%9C%29+sabuncu&btnG=

[25] Zhang, X., Gu, X., Ma, N. (2021). Roll characteristics contributed by a bilge keel using a high-order fractional step finite volume solver. *Ocean Engineering*, 240, 109935. https://doi.org/10.1016/j.oceaneng.2021.109935

[26] IMO. (2006). Interim Guidelines for Alternative Assessment of the Weather Criterion. *International Maritime Organization*, *MSC. 1/Circ. 1200*. https://scholar.google.com/scholar?hl=id&as_sdt=0%2C5&q=Interim+Guidelines+for+Alternative+Assessment+of+the+Weather+Criterion&btnG=

[27] Lewandowski, E. M. (2011). Comparison of Some Analysis Methods for Ship Roll Decay Data. *12th International Ship Stability Workshop*, 325-330. https://doi.org/http://hitech.technion.ac.il/feldman/

[28] Avci, A. G. & Barlas, B. (2019). An experimental investigation of interceptors for a high-speed hull. *International Journal of Naval Architecture and Ocean Engineering*, 11, 256-273. https://doi.org/10.1016/j.ijnaoe.2018.05.001

[29] Molland, A. F., Turnock, S. R. & Hudson, D. A. (2011). *Ship resistance and propulsion* (1st ed.). Cambridge University Press. https://www.cambridge.org/9780521760522; https://doi.org/10.1017/CBO9780511974113

[30] ITTC. (2002). Recommended Procedures and Guidelines: Testing and Extrapolation Methods Resistance Uncertainty Analysis, Example for Resistance Test. *International Towing Tank Conference*, *7.5-02-02-02*. https://ittc.info/media/1818/75-02-02-02.pdf

[31] Indiaryanto, M., Mujahid, A. S., Setyanto, T. A. & Puryantini, N. (2020). Hull Form Factor Prediction of Mini Submarine Model Using Prohaska Method. *EPI International Journal of Engineering*, 3(2), 160-164. https://doi.org/10.25042/epi-ije.082020.12

[32] Katayama, T., Matsuoka, M., Adachi, T. & Ikushima, K. (2019). Effects of half breadth to draught ratio of hull underwater surface on bilge-keel roll damping component. *Ocean Engineering*, 188. https://doi.org/10.1016/j.oceaneng.2019.106283

[33] Asis, M. A., Paroka, D., Asri, S. & Syam, M. A. (2020). Effect of Bilge Keels Position on Roll Motion Performance of Traditional Wooden Boat. *International Journal of Marine Engineering Innovation and Research*, 5(3), 190-197. https://doi.org/10.12962/j25481479.v5i3.7728

[34] Kim, N., Kim, Y. J. & Ha, Y. (2015). Experimental Study of the Free Roll Decay Test for the Evaluation of Roll Damping Coefficients. *Journal of the Society of Naval Architects of Korea*, 52(6), 460-470. https://dx.doi.org/10.3744/SNAK.2015.52.6.460